Two Dimensional DCT/IDCT Architecture

Authors: A. Aggoun and I. Jalloh

Address: Faculty of Computing Sciences and Engineering.

De Montfort University, The Gateway Leicester LE1 9BH.

Contact: Dr. A. Aggoun

Tel: +44 (0)116 2577055

Fax: +44 (0)116 2577692

Email: **aggoun@dmu.ac.uk**

Abstract:

A new fully parallel architecture for the computation of a two-dimensional (2D) discrete cosine transform (DCT), based on the row-column decomposition is presented. It uses the same one-dimensional (1D) DCT unit for the row and column computations and (N^2+N) registers to perform the transposition. It possesses features of regularity and modularity, and is thus well suited for VLSI implementation. It can be used for the computation of either the forward or the inverse 2D DCT.

Each 1D DCT unit uses N fully parallel vector inner product (VIP) units. The design of the VIP units is based on a systematic design methodology using radix-2^n arithmetic, which allows partitioning of the elements of each vector into small groups. Array multipliers without the final adder are used to produce the different partial product terms. This allows a more efficient use of 4:2-compressors for the accumulation of the products in the intermediate stages and reduces the numbers of accumulators from N to 1. Using this procedure, the 2D DCT architecture requires less than N^2 multipliers (in terms of area occupied) and only 2N adders. It can compute a N×N-point DCT at a rate of one complete transform per N cycles after an appropriate initial delay.

Introduction:

The discrete cosine transform (DCT) has emerged as the most popular transform for many image/video compression applications owing to its near optimal performances compared to the statistically optimal Karhunen-Loeve transform [1]. Its energy compaction efficiency is also greater then any other transform. The 2D DCT, in particular, is one of the major operations in current image/video compression standards [2-5]. It is today the most widely used orthogonal transform for applications including videophone, video conferencing and high definition television.

The 2D DCT is computationally intensive and as such there is a great demand for high speed, high throughput and short latency computing architectures. Due to the high computation requirements, the 2D DCT processor design has been concentrated on small nonoverlapping blocks (typical 8x8 or 16x16). Many 2D DCT algorithms have been proposed to achieve reduction of computational complexity and thus increase the operational speed and throughput. The various algorithms and architectures for the 2D DCT can be divided into two categories: the row-column decomposition methods and the non-row-column decomposition methods.

Several hardware design methods for the implementation of the 2D DCT have been developed in recent years [6-9]. Hsia *et. al* [6] reported an algorithm and architecture to calculate the 2D inverse DCT (IDCT) directly by skipping the zero DCT coefficients, since they do not affect the transform results of the IDCT. The IDCT algorithm is realised by a pipelined architecture and modular design and it utilises pipelined combinational multipliers to decrease the critical path. The implementation uses relatively less hardware to achieve sufficient speed for real applications. It achieves an average pixel rate varying from 150 MHz to a maximum pixel rate of 400 MHz when using a 50 MHz clock. The main advantage of the architecture is that it uses a lower operation frequency to obtain a very high pixel rate. However, the disadvantage of this

architecture is that it can only perform the inverse DCT. This is because it utilises the fact that in many image coding systems, most of the DCT coefficients are quantised to zeros and that in interframe coding the nonzero coefficients is even smaller due to the motion compensation in sequential images. As such this system cannot be used to implement both the DCT and IDCT using the same hardware.

Chiang *et. al* [7] reported a 2D DCT/IDCT architecture which utilises the overlapped row-column operation, instead of the transpose memory, in order to reduce the total latency of the structure. The core processor is organised into two cascaded 1D DCT/IDCT units and one control unit. The multiplication block is implemented by using look-up tables. In order to reduce the size of the table, the precalculated partial products of the DCT/IDCT coefficients and the input data are stored in two separate tables. By avoiding the use of multipliers and the transpose RAM the architecture can achieve an operation speed of up to 100 MHz. The disadvantage of this architecture is that different structures are used for the computation of the two 1D DCT blocks.

Fernández *et. al* [8] reported an 8×8 2D DCT processor using the row-column decomposition method, based on the residue number system (RNS). The processors utilise a fast cosine transform algorithm that requires a single multiplication stage for each signal path. Thus each 1D DCT block consists of 14 multipliers and 32 adders and subtractors. Linear combinations of the DCT coefficients are precalculated and stored in ROMs, thus the DCT can be calculated with look-up table multipliers. The transposition unit consists of an 8×8 matrix of registers and multiplexers interconnected to allow the transposition of parallel input data. One of the drawbacks of this system is the practical implementation of RNS-based systems, which possesses serious limitations in the conversion stage. RNS-to binary conversion requires the use

of 32-bit (since the input data and the selected moduli are 8-bit width) word-length adders and large multipliers thus resulting in more hardware and degradation of system performance.

Chang and Wang [9] reported an implementation of the 2D DCT/IDCT based on the row-column decomposition and uses a systolic array without the matrix transposition hardware. The system is achieved in three steps and requires N^2 multipliers and N^2+3N adders. With a throughput rate of one N×N-point DCT per N cycle and a pixel rate of about 320MHz, it has a good area-time performance and it is very attractive for very high-speed applications. However, the significant drawbacks in this work is that the architecture is not modular, it uses different structures to achieve the two 1D DCT blocks and different structures for computing the forward and the inverse 2D DCT.

In this paper, a new fully parallel 2D DCT/IDCT architecture using the linear systolic matrix-vector without the RAM based matrix transposition is presented. It is shown that the architecture is highly modular, parallel and can be used to compute both the forward and the inverse 2D DCT. Finally, it is shown that the proposed architecture enables the realisation of the 2D DCT with a relatively smaller hardware compared to the conventional approaches, and it also results in an extremely regular structure such that its realisation is very simple. A new transposition matrix is introduced which uses (N^2+N) registers and N (N:1) multiplexers. This allows the reading of N output coefficients from the 1st 1D DCT and the feeding of N coefficients to the 2nd 1D DCT in a pipelined fashion. Also, a systematic methodology, which allows the design the vector inner products used to implement the matrix-vector multiplier is presented. It is based on the radix-2^n arithmetic which allows partitioning of the operands to n-bit digits each and hence providing the designer with more flexibility between throughput rate and hardware cost, by varying the digit-size n, the pipelining level and also the type of architecture. In this paper, the radix-$2^{B/4}$ vector inner product architecture is described and is used within the 2D DCT

5

architecture, where B is the data wordlength. The resulting 2D DCT architecture is compared to previously reported architectures.

1. The 2D DCT Algorithm

For a given 2D spatial data sequence $\{X_{ij}; i, j = 0, 1, \ldots, N\text{-}1\}$, the 2D DCT data sequence $\{Y_{pq}; p, q = 0, 1, \ldots, N\text{-}1\}$ is defined by:

$$Y_{pq} = E_p E_q \frac{2}{N} \sum_{i=0}^{N-1} \sum_{j=0}^{N-1} X_{ij} \cos\left[\frac{(2i+1)p\pi}{2N}\right] \cos\left[\frac{(2j+1)q\pi}{2N}\right] \tag{1}$$

where

$$E_x = \begin{cases} 1/\sqrt{2}, & x = 0 \\ 1, & x \neq 0 \end{cases}$$

The forward and inverse transforms are merely mappings from the spatial domain to the transform domain and vice versa. The DCT is a separable transform and as such, the row column decomposition can be used to evaluate equation (1). Denoting: $\cos\left[\dfrac{(2h+1)l\pi}{2N}\right]$ by c_{lh}

and neglecting the scale factor $\dfrac{2}{N} E_p E_q$, the column transform can be expressed as:

$$Y_{pq} = \sum_{j=0}^{N-1} Z_{pj} c_{qj}, \quad p, q = 0, 1, 2, \ldots, N-1 \tag{2}$$

and the row transform can be expressed as:

$$Z_{pj} = \sum_{i=0}^{N-1} X_{ij} c_{pi}, \quad p, j = 0, 1, 2, \ldots, N-1 \tag{3}$$

In order to compute an N x N-point DCT (where N is even), N row transforms and N column transforms need to be performed. However, by exploiting the symmetries of the cosine function, the number of multiplications can be reduced from N^2 to $N^2/2$. In this case, each row transform given by equation (3) can be written as matrix-vector multipliers via,

6

$$Z_{pj} = \sum_{i=0}^{N/2-1}[X_{ij} + (-1)^p X_{(N-1-i)j}]c_{pi} \tag{4}$$

Using a matrix notation, for N=8, equation (4) can written as

$$\begin{bmatrix} Z_{00} \\ Z_{20} \\ Z_{40} \\ Z_{60} \end{bmatrix} = \begin{bmatrix} c_{00} & c_{01} & c_{02} & c_{03} \\ c_{20} & c_{21} & c_{22} & c_{23} \\ c_{40} & c_{41} & c_{42} & c_{43} \\ c_{60} & c_{61} & c_{62} & c_{63} \end{bmatrix} \begin{bmatrix} X_{00} & + & X_{70} \\ X_{10} & + & X_{60} \\ X_{20} & + & X_{50} \\ X_{30} & + & X_{40} \end{bmatrix} \tag{5}$$

$$\begin{bmatrix} Z_{10} \\ Z_{30} \\ Z_{50} \\ Z_{70} \end{bmatrix} = \begin{bmatrix} c_{10} & c_{11} & c_{12} & c_{13} \\ c_{30} & c_{31} & c_{32} & c_{33} \\ c_{50} & c_{51} & c_{52} & c_{53} \\ c_{70} & c_{71} & c_{72} & c_{73} \end{bmatrix} \begin{bmatrix} X_{00} & - & X_{70} \\ X_{10} & - & X_{60} \\ X_{20} & - & X_{50} \\ X_{30} & - & X_{40} \end{bmatrix} \tag{6}$$

Equations (5) and (6) describe the computation of the even and odd coefficients, for the row transform for N=8, respectively. The computation for the second 1D DCT i.e. the column transform described by equation (2) can also be computed using matrix-vector multipliers similar to that described by equation (4). Hence both the row and column transform can be performed using the same architecture.

The architecture for computing the row transform, for N = 8, is depicted in figure 1. It is based on Step 1 of the systolic array implementation proposed by Chang *et al* [9]. It consists of N/2 adder/subtractor cells for summing and subtracting the inputs to the 1D DCT block as required by equation (4). The pair of inputs X_{ij} and $X_{(N-1-i)j}$ enters the $(i+1)^{th}$ adder/subtractor cell. In the proposed architecture, all the pairs of input data enter the adder/subtractor cells at the same time. Figure 1 shows that the architecture also consists of N vector inner products, where half are used for the added pairs as described by equation (5) and the other half for the subtracted pairs as described by equation (6). Each vector inner product consists of N/2 multiplier/accumulator cells. Each cell stores one coefficient c_{pi} in a register and evaluates one specific term over the summation in (4). The multiplications of the terms c_{pi} with the corresponding data are performed simultaneously and then the resulting products are added together in parallel. This

addition is carried out using carry save arithmetic modules incorporated within the multipliers structure as will be described is section 4.

2.   VLSI Architecture for the 2D DCT

The 1D DCT module accepts N samples of the input data in parallel and produces N coefficients in parallel. The proposed 2D DCT architecture is shown in figure 2 for N=8. It is based on the row-column algorithm and is divided into three main stages. Stage one and stage three computes the row and column transforms, respectively. Both the row and column transforms are implemented using the same 1D DCT module shown in figure 1. The second stage performs the transposition using (N^2+N) registers and N (N:1) multiplexers. The (N^2+N) registers are divided into two sets of $(N^2+N)/2$ skewed registers and the data is fed from one set to the other via the multiplexers. The 1D DCT unit accepts input vectors in parallel and produces the N DCT coefficients in parallel. The N outputs from the row transform are fed into an array of skewed shift registers as shown in figure 2 to enable the reading of only one coefficient from the same output vector at any one time. This achieves the appropriate reordering of the data into the second array of skewed registers. The skewed registers are made of N shift registers with lengths varying from 1 to N, respectively. For simplicity the N shift registers in either arrays of skewed registers are termed R_1^m, R_2^m, …, R_N^m where the lower index specifies the length of the shift register and the upper index, m, specifies either the first or the second array of skewed register for m=1 or 2, respectively. An array of N (N:1) multiplexers is used to send the output data to the correct shift registers in the second array of skewed registers. Each of the outputs from the row transform is fed into one of the shift registers R_1^1, R_2^1, …, R_N^1. Each of the shift registers, R_1^1, R_2^1, …, R_N^1, produces one output every clock cycle which is fed into one of the shift registers, R_1^2, R_2^2, …, R_N^2 via one of the (N:1) multiplexers. Figure 3 shows the utilisation of the skewed registers during the first four cycles. In the first cycle the results of the first 1D

8

DCT are stored in R^1 as shown in figure 3a. During the second cycle, the data from R_1^1 (i.e. Z_{00}) is fed into the shift registers R_N^2 (see figure 3b). In the third cycle the data from R_1^1 (Z_{01}) is fed into R_{N-1}^2 and the data from R_2^1 (Z_{10}) is fed into R_N^2 (see figure 3c). In the fourth cycle, the data from R_1^1 (Z_{02}) is fed into R_{N-2}^2, the data from R_2^1 (Z_{11}) is fed into R_{N-1}^2 and the data from R_3^1 (Z_{20}) is fed into R_N^2 (see figure 3d). This process is continued until the entire data is transferred. At the $(N+1)^{th}$ cycle the data from R_1^1 ($Z_{0,N-1}$) is fed to R_1^2, while the data from R_N^1 ($Z_{N-1,0}$) is fed into R_N^2. At this point, the N point data incoming from the first VIP or register R_1^1 is available at the output of the registers R_1^2, R_2^2, ..., R_N^2 and ready to enter the column transform as shown in figure 4 for N=8. In the following cycle the data from the second VIP or the register R_2^1 is ready to enter the column transform, while the data from the first VIP or register R_1^1 is being processed by the second 1D DCT. This process continues till all the remaining coefficients in the skewed registers R^2 have entered the column transform. Hence after an initial delay of (N+1) cycles, the proposed architecture will output N 2D DCT coefficients every clock cycle. Whilst the 1D DCT coefficients stored in the array of skewed registers R^2 are being processed by the second 1D DCT block, the transfer from the first 1D DCT block into the array of the skewed registers R^2 via the array of skewed registers R^1 and the array of multiplexers continues until all the input data has been processed.

For N=8, a 3-bit control signal is required to enable the 8:1 multiplexers to select one of the eight input words. During the first cycle of the transfer of data from R^1 to R^2, the first multiplexer from the right will select its port 1 as its output. In the second cycle, the second multiplexer on the right will select port 1 as its output while the first multiplexer from the right will select port 2 as its output and so on. Hence, the control signal is connected to all multiplexers through delay elements as shown in figure 2.

3. Radix-2^n Vector inner product algorithm:

In this section the design of a fully parallel architecture for computing the product of two vectors is presented. The proposed architecture of the vector inner product is derived from a design methodology using radix-2^n arithmetic reported by A. Aggoun *et.al.* [10]. To demonstrate the proposed methodology, the inner product of the vectors $U_i = c_{pi}$ and $V_i = X_{ij} + (-1)^p \cdot X_{(N-1-i)j}$ described by equation 4 is considered. Using the radix-2^n arithmetic and assuming unsigned numbers, U_i can be divided into K digits of n-bit each and can be written as [10],

$$U_i = \sum_{r=0}^{K-1} u_{ri} 2^{rn}$$

(7)

where u_{ri} represents the rth digit of the U_i. The vector inner product can be computed according to the following equation [10],

$$W = \sum_{i=0}^{N/2-1} \sum_{r=0}^{K-1} (u_{ri} \cdot V_i) 2^{rn}$$

(8)

It is worth noting that the path of the generation of the partial products is independent of the propagation path of the accumulating partial sums as shown in figure 5. In the proposed radix-2^n design methodology, any composite summations, as that given in Equation (8), can be combined into one. Hence equation 8 can be rewritten as,

$$W = \sum_{s=0}^{NK/2-1} W_s$$

(9)

where $W_s = u_{ri} \cdot V_i \cdot 2^{rn}$ and s=iK+r. As a result, the partial products can be carried out simultaneously and the resulting N/2×K sums are added together in parallel. This can be carried out using carry save arithmetic and a final carry lookahead adder.

The advantage of describing the vector inner product using the radix-2^n algorithm and merging summations, as in equation 9, is to provide designers with more flexibility not only by varying the

10

digit size n, but also in the way the accumulation of the partial sums is carried out. This is evident when it is realised that there are numerous ways in which the summation in equation (9) can be decomposed; the decomposition in equation (8) being only one of those. In other words, the sum in equation (9) can be split into several nested sums where each sum can be carried out in an independent way using either a tree or a liner structure. Each one of these different mappings would lead to a different architecture with its own are-time complexity. As an example, the conventional word level VIP architecture is obtained by splitting the summation in equation (9) into the two summations in equation (8) and performing the summation over index r first. In this paper, a new implementation is proposed which is derived without splitting the summation in equation (9).

4. Design of a two's complement parallel vector inner product:

In this section the architecture of a two's complement radix-$2^{B/4}$ VIP, where B is the data wordlength, is discussed. The radix-2^n VIP algorithm described by equation (8) assumes unsigned numbers. In what follows, the two's complement array multiplication proposed by Baugh and Wooley [11] is adapted to two's complement radix-2^n multiplication. Let consider the multiplication of two B-*bit* two's complement numbers, where the multiplier and the multiplicand, U_i and V_i, are written in the form

$$
\begin{aligned}
U_i &= -u_i^{B-1} 2^{B-1} + \tilde{U} \\
V_i &= -v_i^{B-1} 2^{B-1} + \tilde{V}
\end{aligned}
\tag{10}
$$

where $\tilde{U}$ and $\tilde{V}$ are (B-1)-*bit* positive number comprising the B-1 least significant bits of U_i and V_i, respectively, and u_i^{B-1} and v_i^{B-1} are their most significant bits. Following the same procedure as in [10] and [12], the multiplication of two B-*bit* two's complement numbers, U_i and V_i, can be written in a form involving only positive partial products provided that all partial products which involve a sign bit and a nonsign bit are complemented. The final product is then obtained by adding a fixed correction term to the final result, viz.,

$$U_i \cdot V_i = (u_i^{B-1} \cdot v_i^{B-1}) \cdot 2^{2B-2} + \tilde{U}_i \cdot \tilde{V}_i + (\overline{\tilde{U}_i \cdot v_i^{B-1}} + \overline{\tilde{V}_i \cdot u_i^{B-1}}) \cdot 2^{B-1} + 2^B - 2^{2B-1} \qquad (11)$$

Two's complement representation is adapted to normal multiplication by simply replacing the AND with a NAND gate for all the partial product involving the sign bits, u_i^{B-1} and v_i^{B-1}, as can be seen from equation (11), except for the product $u_i^{B-1} \cdot v_i^{B-1}$, which is carried out using an AND gate.

In the new implementation, each of the N/2×K products, W_s, is computed using the array multiplier shown in figure 6 for B=16 and K=4. As can be seen in figure 6, the two top carry save adders (CSAs) and the column of full adders (FAs) involving the sign bit v_i^{B-1} required in conventional array multipliers, are removed since they have empty bit positions. However, on the right hand side of each array a column of half adders (HAs) is needed to add the two bits $u_{ri}^0 \cdot v_i^1$ and $u_{ri}^1 \cdot v_i^0$ and propagate the carry bits from the top to the bottom as shown in figure 6. Each array multiplier produces a (5B/4-1)-bit sum word and a B-bit carry word for K=4. As a result, N×K words are fed into the accumulation path and arranged with respect to their significance as shown in figure 7 for N/2=K=4.

The addition of the term -2^{2B-1} is taken care of by adding a 1 to the most significant bit of the result and the term 2^B by adding a 1 to the (B+1)th column of the final result [4]. This is achieved by extending the carry word of the products, $u_{K-1,i} \cdot V_i$, by one nonzero bit as shown in figures 7 and 8 for the -2^{2B-1} term and feeding a one into the empty bit position of the AND gated FA, ($u_{0,i}^2 \cdot v_i^{B-2}$), of the array multiplier which computes the product $u_{0,i} \cdot V_i$ for the term 2^B, as shown in figure 6 for B=16.

The partial sums and carries from all the N/2×K multipliers are accumulated together in parallel using carry save arithmetic implemented with 4-2 compressors as shown in figure 8. The partial

sums and carries are repartitioned into digits of B/4-bit each as shown in figure 7. All the terms with the same significance, k, are added together using an array of B/4-bit 4:2-compressors as shown in figure 9 for k=4. The B/4-bit 4:2-compressors are obtained by interconnecting two B/4-bit CSAs with fast input and output. The output from the first CSA with the longest path (i.e. path through two XORs) is fed into the carry input of the second CSA. This makes the total delay through the 4:2-compressors equivalent to three XORs. The critical path in the accumulation of the partial sum and carry terms consists of four B/4-bit 4:2-compressors which is obtained for k=4 as shown in figure 9. Hence, the longest delay in the accumulation of the all the sum and carry terms is equivalent to that of six FAs.

It is worth mentioning that carry bits are propagated between the array of 4-2 compressors from right to left. Let P_k be the array used for the accumulation of all terms with the same significance, k. For k < 4, the output carries from the array P_k are fed directly into the carry inputs of the array P_{k+1}. However, for k $\geq$ 4, the number of carries generated by the array P_k is greater than the number of carry inputs available to the array P_{k+1}. As a result, extra FAs and/or HAs are required to accommodate the extra carries. This is shown as an example in figure 10 for k=5, where the array P_5 takes carries from P_4. Each 4-2 compressor produces two 1-bit carry outputs and has one 1-bit carry input. Furthermore, all the 4-2 compressor of the arrays P_k, except the ones in the top, will have an extra two 1-bit empty position, which can accommodate carry bits. To compress 24 bits into 2 bits, the array P_5 would require a total of eleven 4-2 compressors, where six are in the top row and five in remaining stages. Hence the array P_5 can take up to 21 carry bits. However, the array P_4 will produce a total of 30 carry bits, one of which is fed to the carry look ahead adder and the remaining 29 are fed into the array P_5. To take care of the remaining eight carry bits, a 1-bit and a B/4-bit 4-2 compressors are added to the array P_5 as shown in figure 10. Similarly, 4-2 compressors are added to the arrays P_6 and P_7 to accommodate the extra carry bits from the array P_5 and P_6, respectively.

5. Performance analysis:

In this section, the performance of the proposed parallel 2D DCT architecture is compared with the design proposed in [9]. The proposed architecture employs 2N vector inner product units and parallel-in parallel-out I/O form. Each vector inner product unit are implemented using N/2 parallel multipliers without the final adder. The addition of the partial product from the N/2 multipliers is carried out in parallel and is embedded within the structure of the parallel multipliers. One of the operands of each multiplier is divided into four groups, which produces four carry words and four sum words. The total of 4N words are added together using carry save arithmetic implemented with arrays of 4-2 compressors. The 4-2 compressors within each array are arranged in a tree structure and used to add terms with the same significance. In what follows $A_{CSA}(N,B)$ denotes the hardware cost required by the addition of the 2N (5B/4-1)-bit partial sum words and the 2N B-bit carry words using carry save arithmetic. Assuming a B-bit input data, one $(2B+\log_2(N/2)+1)$-bit carry lookahead adder is required for each vector inner product unit. The 1D DCT unit also requires N B-bit adder or subtractor units to add or subtract pairs of input data before being fed into the vector inner products. Hence, the total cost of the 1D DCT unit is given by

$$A_{1DDCT}(B,N) = N\left[\frac{N}{2}\left(B^2A_{AND} + B(B-2)A_{FA}\right) + A_{CLA}\left(2B + \log_2\left(\frac{N}{2}\right) + 1\right) + A_{CLA}(B) + A_{CSA}(N,B)\right]$$

where A_{AND}, A_{FA} and $A_{CLA}(B)$ are the area taken by an AND, an FA and a B-bit carry lookahead adder. Assuming that the data is truncated to B-bit before entering the transposition buffer, which is made of $(N^2+N)/2$ registers and N B-bit 8:1 multiplexers. Each 8:1 multiplexers could be implemented using a tree of seven 2:1 multiplexers. The cost of a B-bit 2:1 multiplexer is that of 3B AND gates. Hence the total cost of the buffer transposition unit is given by

$$A_{buffer}(B,N) = 21NBA_{AND} + \frac{N^2+N}{2}A_{Reg}(B)$$

where $A_{Reg}(B)$ is the cost of a B-bit register. The total cost of the proposed 2D DCT architecture is that of two 1D DCT units plus that of the buffer transposition unit, via

$$A_{2DDCT}(B, N) = 2A_{1DDCT}(B, N) + A_{buffer}(B, N)$$

The 2D DCT architecture in [9] consists of three stages. The first stage consists of N B-bit adder or subtractor units and N vector inner products. In conventional DCT implementation, the vector inner products are usually implemented with a linear array of multiplier accumulators. To carry out a fair comparison the parallel multipliers are implemented using the same structure as in [12]. In this case, each vector inner product unit will require N/2 arrays of B/4-bit 4-2 compressors and N/2 (2B+1)-bit carry lookahead adders. Each array of 4-2 compressors will have a cost $A_{CSA}(1,B)$. Also, N/2 (2B+1)-bit delay elements are required to be placed at the output of the multiply-accumulator cells. Furthermore, N(N-2)/4 B-bit registers are required at the input of stage 1. Hence, the total cost of the first stage of the architecture in [9] is given by

$$A_{stage1}(B, N) = \frac{N^2}{2}\left(B^2 A_{AND} + B(B-2)A_{FA} + A_{CSA}(1, B) + A_{CLA}(2B+1) + A_{Reg}(2B+1)\right)$$
$$+ NA_{CLA}(B) + \frac{N^2 - 2N}{4}A_{Reg}(B)$$

Stage 2 of the architecture in [9] consists of N basic cells plus N(N-2)/4 B-bit registers. Here, it is assumed that the data from the first stage is truncated to B bits. Each basic cell consists of three B-bit registers, two B-bit adder/subtractor units and one B-bit 2:1multiplexers.

$$A_{stage2}(B, N) = N\left(3BA_{AND} + BA_T + 2A_{CLA}(B)\right) + \left(\frac{N^2 + 10N}{4}\right)A_{Reg}(B)$$

The third stage of the architecture in [9] consists of $N^2/2$ cells and $(N^2/2)$ B-bit registers. Each cell consists of a B-bit multiplier, two (2B+1)-bit adders, two 2B-bit registers, two 2B-bit 2:1 multiplexers and one 2B-bit 3:1 multiplexer. Each B-bit multiplier consists of arrays of 4-2 compressors, four B×B/4-bit array multipliers and one (2B+1)-bit adder. Hence the total cost of the third stage is given by

$$A_{stage3}(B,N) = \frac{N^2}{2}\left((B^2 + 26B)A_{AND} + B(B-2)A_{FA} + 3A_{CLA}(2B+1) + A_{CSA}(1,B) + 2A_{\text{Re}g}(2B)\right)$$
$$+ \left(\frac{N^2}{2}\right)A_{\text{Re}g}(B)$$

The total hardware cost of the architecture proposed in [9] for the computation of the forward 2D DCT is

$$A'_{2DDCT} = A_{stage1}(B,N) + A_{stage2}(B,N) + A_{stage3}(B,N)$$

Table 1 shows the area occupied by the proposed 2D DCT architecture and the architecture in [9] for N=4, 8 and 16. The area for each unit in both architectures is computed using the procedure reported in [13], where A_T is the area required in an inverter circuit. It is assumed that $A_{AND}=2A_T$, $A_{FA}=10A_T$ and $A_{Reg}(1)=7A_T$. It can be seen that for N=8 about 33% reduction in the hardware cost has been achieved by the proposed architecture over the architecture in [9].

6. Conclusions

In this paper, a new fully parallel architecture based on row-column decomposition has been proposed for the computation of the 2D DCT. The system involves no memory transposition, and is highly modular and utilises a highly parallel structure to achieve high-speed performance. Due to its widely identical units, it will be relatively easy to implement and very suited to VLSI implementation. It uses two identical units for the computation of the row and column transforms and arrays of shift registers to perform the transposition operation. As compared to the pipelined regular architecture in [9], the proposed architecture achieves the same throughput rate at much lower hardware cost and communication complexities. It also requires a much simpler control than the architecture in [9], which requires shuffling of the input data to allow a relatively simplified architecture for the second and third stages. It is also worth mentioning that in the proposed design, the same architecture can be used for the computation of both the forward and the inverse 2D DCT.

References

[1].   K. R. Rao and P. Yip. *Discrete Cosine Transform; Algorithms, Advantages and Applications*. Academic Press Inc., 1990.

[2].   M. Liou. *Overview of the p × 64 kbits/s Video Coding Standard*. Commun., ACM, vol. 34, no. 4, pp. 59 – 63, Apr. 1991.

[3].   G. K. Wallace. *The JPEG Still Picture Compression Standard*. Commun., ACM, vol. 34, no. 4, pp. 30 – 40, Apr. 1991.

[4].   D. LeGall. *A Video Compression Standard for Multimedia Applications*. Commun., ACM, vol. 34, no. 4, pp. 46 – 58, Apr. 1991.

[5].   ISO/IEC DIS 13818 – 2, *MPEG-2 Video*. Draft Int. Standard.

[6].   S. C. Hsia, B. D. Liu, J. F. Yang and B. L. Bai. *VLSI Implementation of Parallel Coefficient-by-Coefficient Two-Dimentional IDCT Processor*. IEEE Trans. on Circuits and Systems for Video Tech., vol. 5, no. 5, pp. 396 – 406, Oct. 1995.

[7].   J. S. Chiang, Y. F. Chui and T. H. Chang. *A High Throughput 2-Dimensional DCT/IDCT Architecture for Real-Time and Video System*. IEEE Proc. of Int'l Conf. on Electronic Circuits and Systems, vol. 2, pp. 867 – 870, Sept. 2001.

[8].   P. G. Fernández *et. al. Fast RNS-Based 2D-DCT Computation on Field-Programmable Devices*. IEEE Workshop on Signal Processing Systems, pp. 365 – 373, Oct. 2000.

[9].   Y. T. Chang and C. L. Wang. *New Systolic Array Implementation of the 2D Discrete Cosine Transform*. IEEE Trans. on Circuits and Systems for Video Tech., vol. 5, no. 2, Apr. 1995.

[10]. A. Aggoun *et.al.*: 'Bit-level pipelined digit-serial array processors' IEEE Trans. Circuit and Systems, vol. 45, no. 7, pp. 857-868, July 1998.

[11]. R. Baugh and B. A. Wooley. '*A Two's Complement Parallel Array Multiplication Algorithm',* IEEE Trans. Computers, vol. C-22, no. 12, pp. 1045 – 1047, Dec. 1973.

[12]. A. Aggoun. '*Two's Complement Parallel Multiplier'.* Electronic Letters, vol. 34, no. 16, pp. 1570 – 1571, Aug. 1998.

[13]. C. L. Wey and T. Y. Chang: 'Design and analysis of VLSI based parallel multipliers' IEE Proc. E, vol. 137, no. 4, pp. 328-336, 1990.

	Proposed Architecture	Architecture in [9]	Improvement
N=4	$73608A_T$	$99976A_T$	27%
N=8	$281456A_T$	$418144A_T$	33%
N=16	$1099744A_T$	$1544896A_T$	29%

Table 1: Hardware cost of the proposed architecture and that in [9] for a 16-bit wordlength.
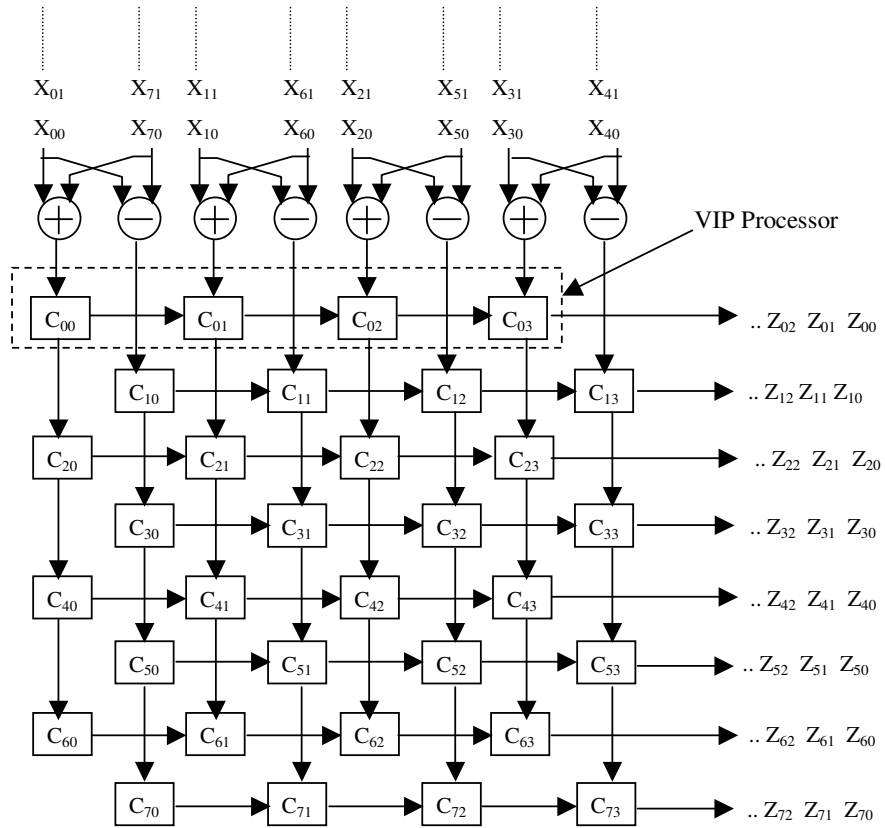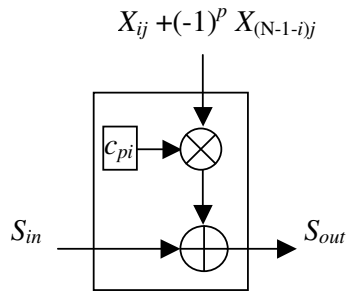
Figure 1: (a) Architecture of a 1D DCT Block for N=8. (b) basic cell.
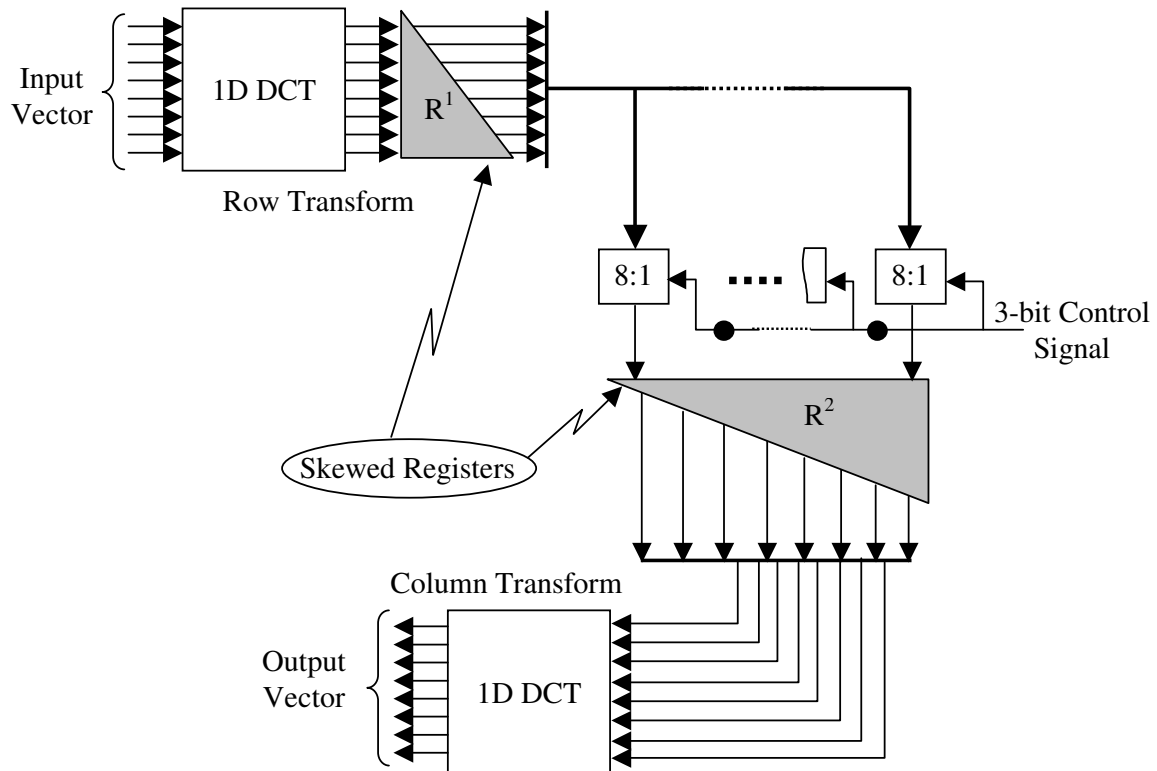
Figure 2: Block diagram of the 2D DCT for N=8.
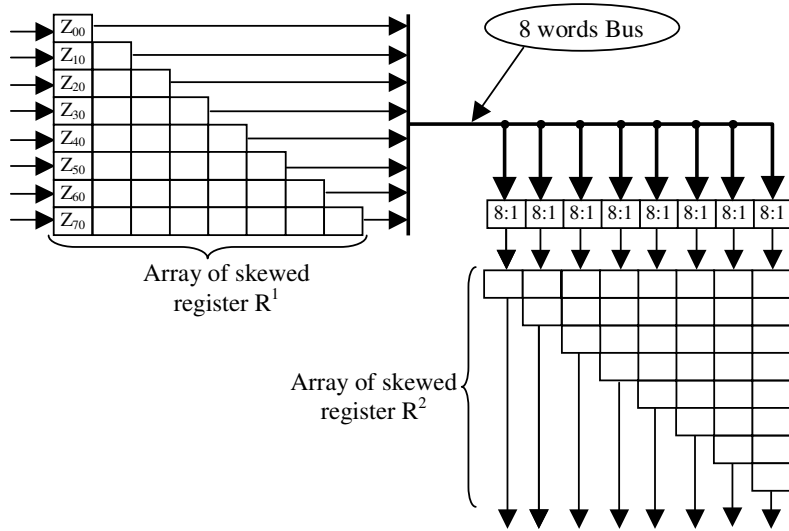
(a) Cycle 1
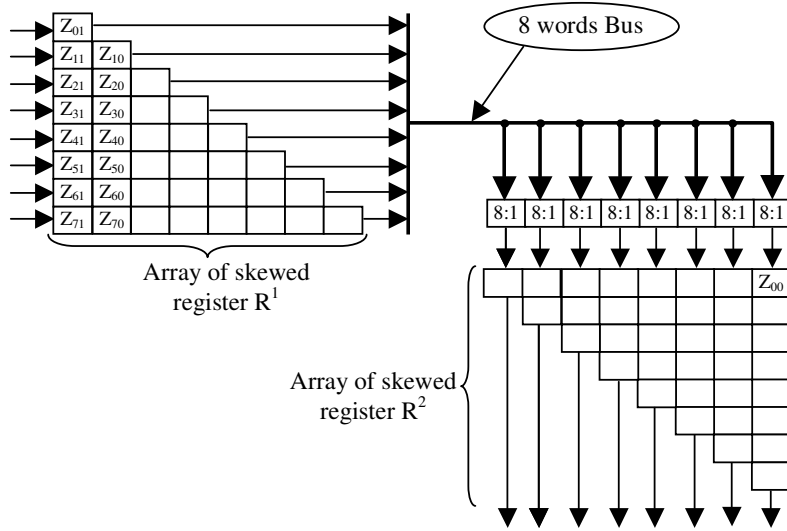
(b) Cycle 2

22
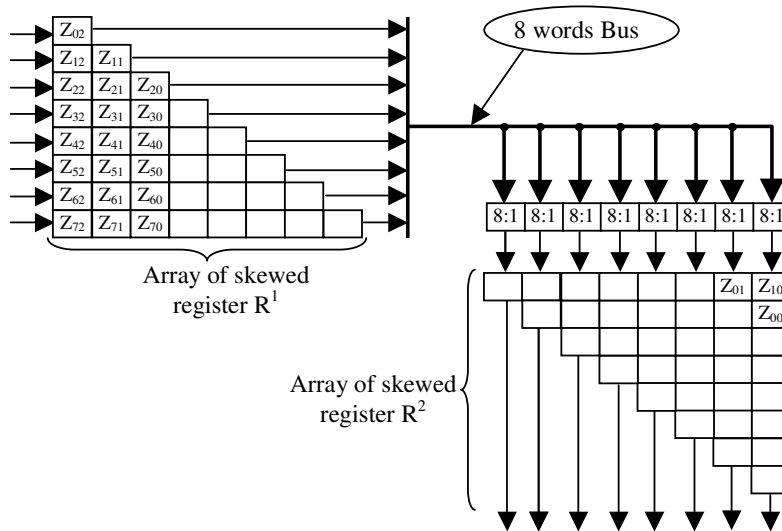
(c) Cycle 3
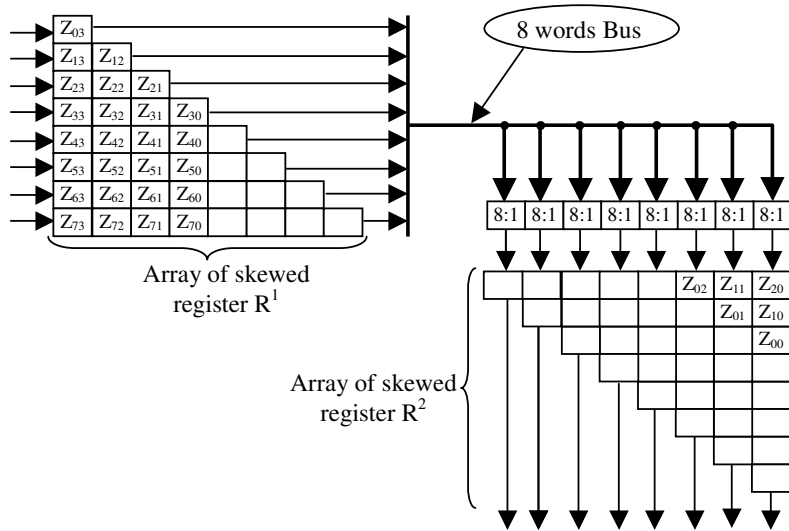
(d) Cycle 4

Figure 3: Utilisation of the skewed registers during the first four cycles.
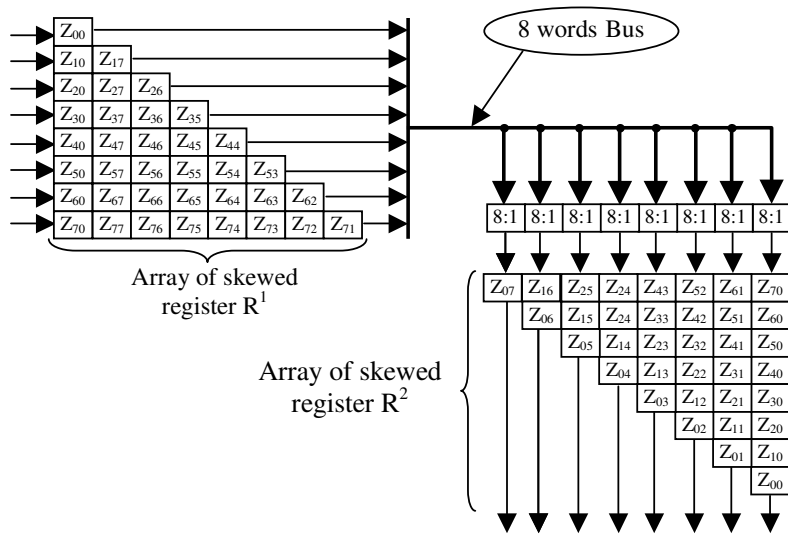
Figure 4: Utilisation of the skewed registers at the 9th cycle for N=8.
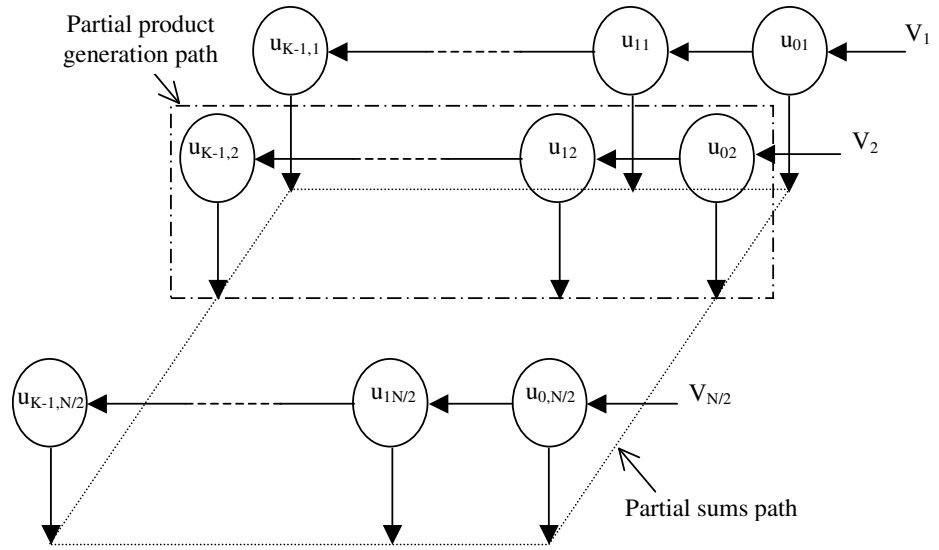
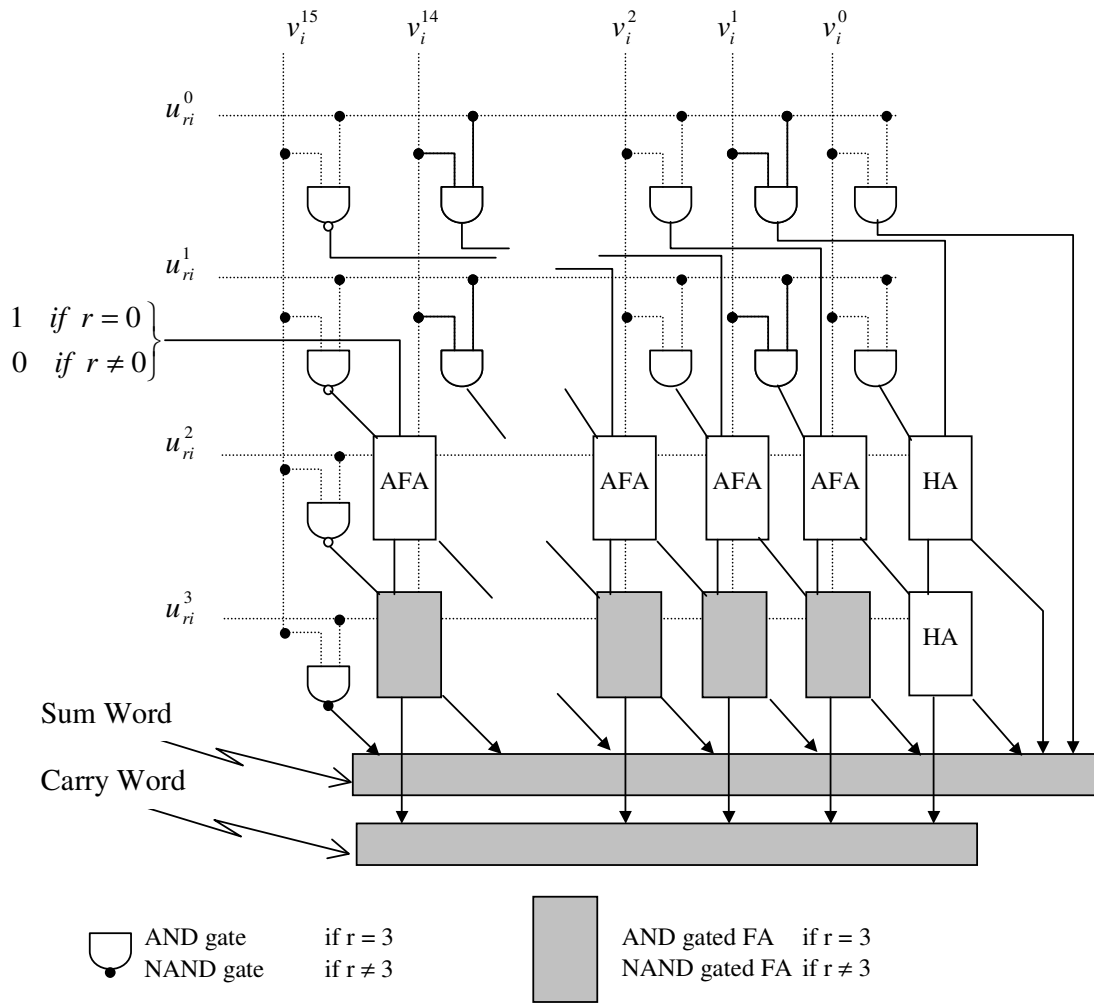Figure 5: Dependency graph of the proposed radix-2^n VIP

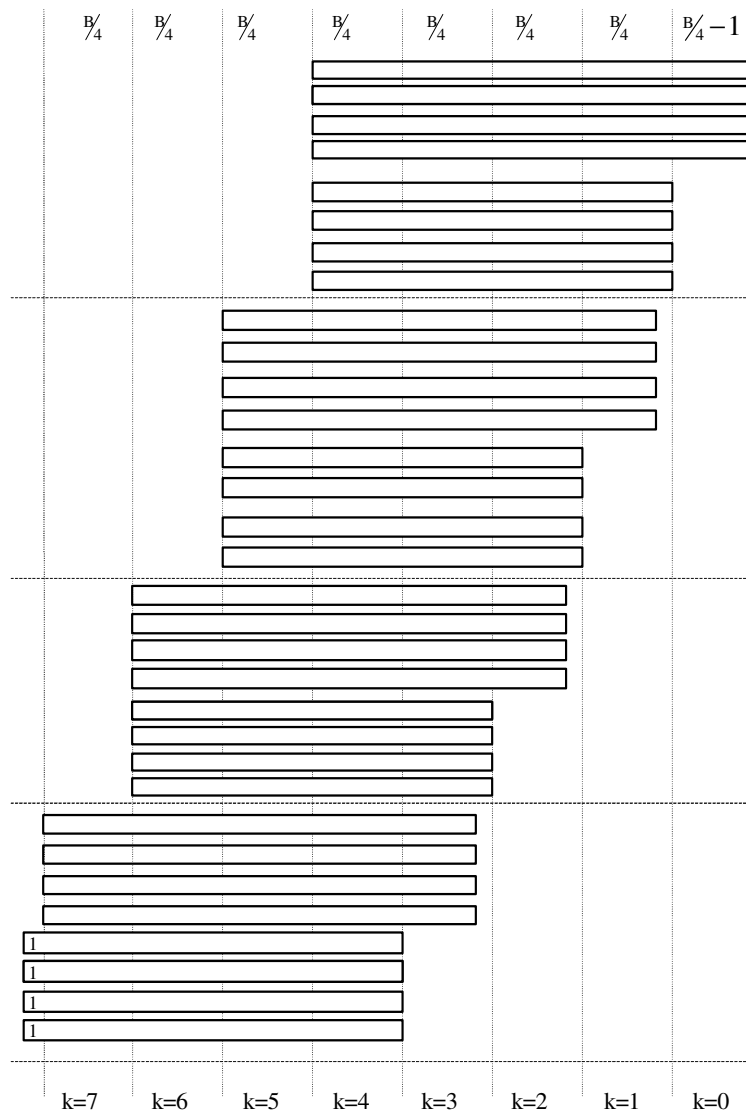Figure 6: Array multiplier used for each of the partial product generation u_{ri} V_i for B=16.

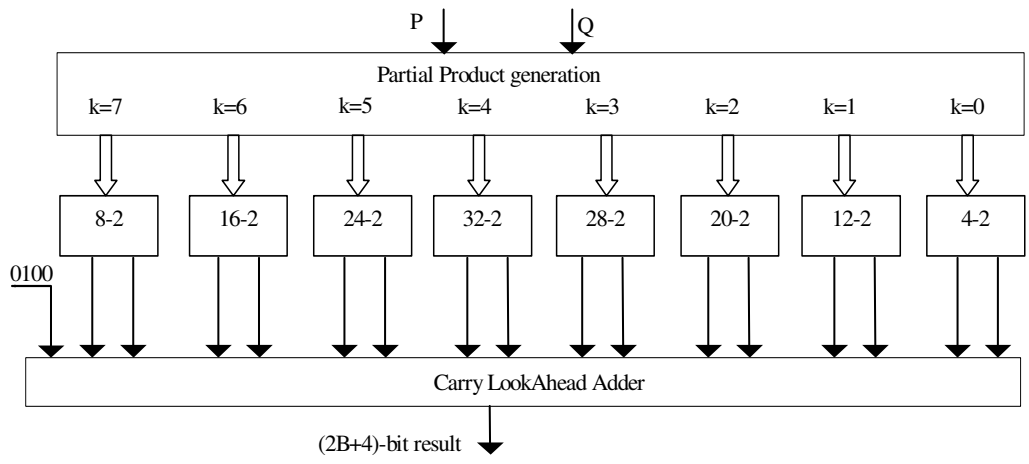Figure 7: Repartitioning of the partial sum and carry words into B/4-bits and their relative bit positions for N=8.

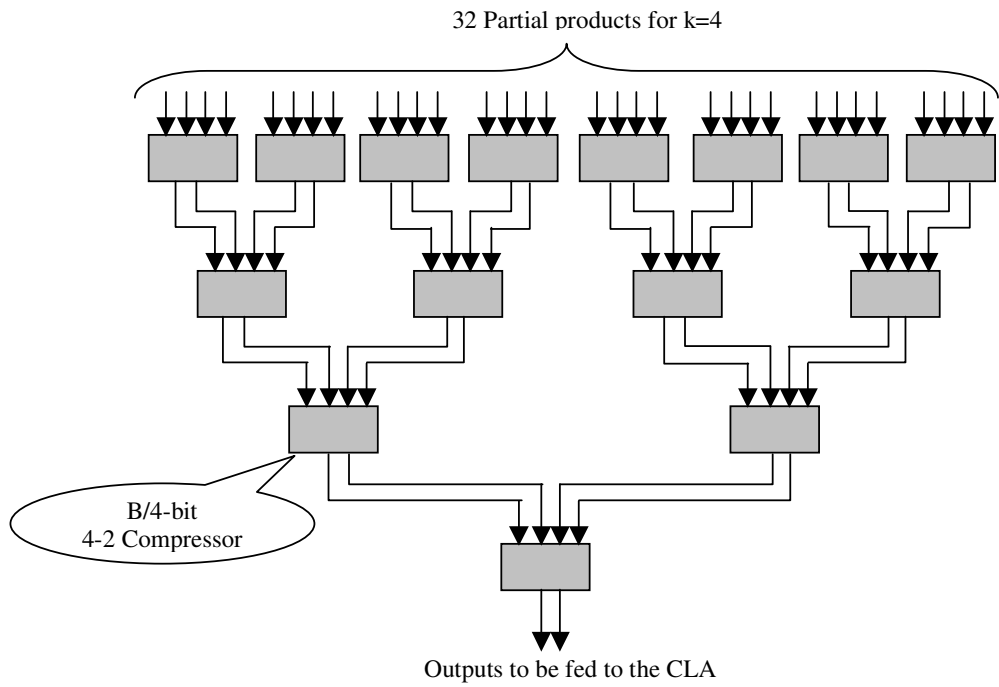Figure 8: Accumulation process of the partial products for N=8

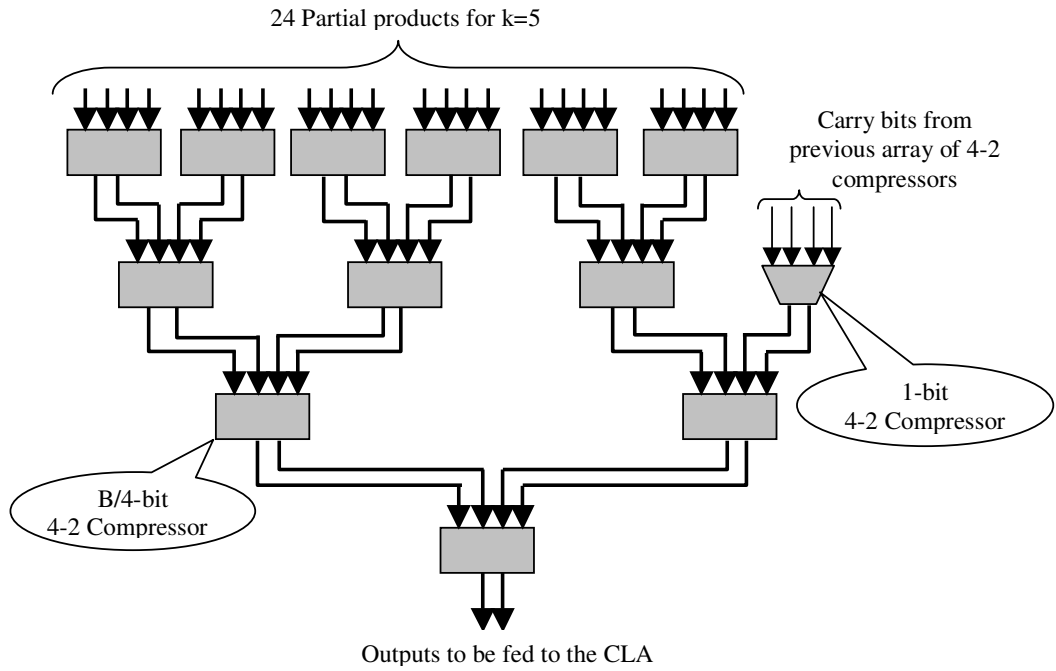Figure 9: Partial products accumulation for N=8 and k=4 using a 32-2 compressor.

24 Partial products for k=5

Carry bits from previous array of 4-2 compressors

1-bit
4-2 Compressor

B/4-bit
4-2 Compressor

Outputs to be fed to the CLA

Figure 10: Partial products accumulation for N=8 and k=5 using a 24-2 compressor.